Progress In Electromagnetics Research, PIER 74, 21–38, 2007

OPTIMAL DESIGN OF DUALBAND CPW-FED G-SHAPED MONOPOLE ANTENNA FOR WLAN APPLICATION

W.-C. Liu

Department of Aeronautical Engineering
National Formosa University
Huwei, Yunlin, Taiwan 632, R.O.C.

Abstract—A dualband coplanar waveguide (CPW)-fed planar monopole antenna suitable for WLAN application is presented in this paper. The antenna resembling as a "G" shape and optimally designed by using the particle swarm optimization (PSO) algorithm can produce dual resonant modes and a much wider impedance bandwidth for the higher band. Prototypes of the obtained optimized antenna have been constructed and tested. The measured results explore good dualband operation with −10 dB impedance bandwidths of 9.7% and 62.8% at bands of 2.43 and 4.3 GHz, respectively, which cover the 2.4/5.2/5.8 GHz WLAN operating bands, and show good agreement with the numerical prediction. Also, good antenna performances such as radiation patterns and antenna gains over the operating bands have been observed.

1. INTRODUCTION

It has been well known that the future communication technology pressingly demands integration of more than one communication system into a limited equipment space. Thus, the future communication terminal antennas will not only be desired to be low-profile lightweight, flush mounted, and single-feed but also need to meet the requirements of dual- or multiband operation for sufficiently covering the possible operating bands. So far, many antenna designs with enhanced dual- or multiband operation capabilities have been developed and presented, which include the planar inverted-F antennas (PIFAs) [1–3], the chip antennas [4, 5], the planar monopole antennas [6–8], and the coplanar waveguide (CPW)-fed antennas [9–12]. However, among these antennas, the CPW-fed monopole antennas

have particularly received much more interest than others owing to their potential in providing various required radiation features of dual- or multiband, broad bandwidth, simple structure of a single metallic layer, and easy integration with system circuit board.

Considering that the dual- or multiband antenna design usually involves many geometry or material parameters, which may be discrete, and often include constrains in allowable values. To optimize such antennas to closely approximate desired resonant performance is similar to searching the global solution from a multidimensional solution space. Therefore, many stochastic evolutionary search techniques, such as simulated annealing (SA) and genetic algorithms (GAs), have been employed and shown successfully in design of such an antenna [13, 14]. Especially, the particle swarm optimization (PSO), based on resembling the social behavior of a swarm of bees to search the location with the most flowers in a field, has recently been found to be an invented high performance optimizer for solving multidimensional discontinuous problems [15]. This technique is somewhat similar to GAs and heuristic algorithms, but requires easier programming formulation and less computational spending. Thus, the PSO has been successfully applied to a variety of fields, especially, used in conjunction with the numerical electromagnetic solver to antenna design and optimization [16–20]. Like an evolutionary algorithm, the PSO, based on the processes of "movement" and "intelligence" in a heuristic system, is an iterative optimization procedure to lead ultimately to the closest approximation to the antenna specification with minimal foresight or pre-conditioning on the part of the designer. The immense power of the technique is its ability to satisfy a performance criterion without any *a priori* knowledge of candidate configurations, and the facility for finding the global optimum result.

In this paper, we will examine the use of a PSO to search a CPW-fed G-shaped planar monopole antenna with optimal dualband operation simultaneously suitable for use in the 2.4/5.2 GHz wireless local area network (WLAN) applications. The geometry parameters of the proposed antenna, including the dimensions of the G-shaped strip structure, the sizes of the coplanar ground planes, and the spaces between the ground plane to either the G-shaped strips or the CPW feeding line, were all manipulated by the PSO to achieve good dualband operation. In addition, the IE3D$^{\text{TM}}$ electromagnetic solver was used to predict the performance of each antenna designed by the PSO. Details of the antenna design are described, and prototypes of the PSO-optimized antenna for dualband operation have been constructed and tested. Also, effects of the G-shaped size on the antenna performance and comparison between the theoretical and experimental results of

the optimal antenna are all examined and discussed.

2. THE PSO ALGORITHM

In the PSO algorithm, each potential solution in an n-dimension space is represented as a particle with a position vector and a moving velocity represented as $\mathbf{x}$ and $\mathbf{v}$, respectively, and will keep track of its position, which is uniformly spread for each dimension in the solution space, bounded by $[\mathbf{x}_{i,n}^{\min}, \mathbf{x}_{i,n}^{\max}]$, to avoid particles flying out of the physically meaningful solution space. Once the position for any particle violates the limit, one of the there proposed control techniques, the "absorbing wall", the "reflecting wall", and the "invisible wall", can be selected for use [17]. In addition, an associated value for each particle is evaluated in accordance with a function called the *fitness function*, which is critically defined and configured from a consideration of the search objective. Thus, the position of the individual best solution that the ith individual particle has achieved so far and that of the best solution that has been obtained among all the particles in the population so far are known as the personal best (denoted as $\mathbf{x}_i^{best}$) and the global best (denoted as $\mathbf{x}^{best}$), respectively, and both are stored for generating the new velocity of ith particle. The PSO algorithm is iterative and the implementation steps of a typical PSO algorithm can be summarized as follows.

Step 1: The PSO begins by generating a population (called swarm) of particles at random to explore a broad population of possible solutions in the entire search space.

Step 2: According to the defined fitness function, the fitness of each particle is evaluated to further obtain the personal best ($\mathbf{x}_i^{best}$) and the global best ($\mathbf{x}^{best}$) particles for use in producing the new velocity and position for each particle. In addition, whether the algorithm stops is also determined during this step from checking that if an acceptable target solution or a set maximum number of search iterations has been achieved.

Step 3: If the algorithm does not stop, each particle adjusts its velocity according to its own experience and the position of the best of all particles to move toward the best solution. The new velocity $\mathbf{v}_i(\mathbf{t})$ for particle i is updated by

$$\begin{aligned} v_i(t) &= w \cdot v_i(t) + c_1 * \text{rand}() * \left(x_i^{best}(t) - x_i(t)\right) \\ &\quad + c_2 * \text{rand}() * (x^{best}(t) - x_i(t)) \end{aligned} \tag{1}$$

Based on the updated velocities, a new position for particle i is thus computed according the following equation:

$$x_i(t) = x_i(t) + v_i(t) \tag{2}$$

Apparent from this equation, the new velocity is related to the old velocity weighted by w and also associated to the position of the particle itself and that of the global best one by factors c_1 and c_2, respectively. c_1 and c_2 are therefore referred to as the cognitive and social rates, respectively, because they represent the weighting of the acceleration terms that pull the individual particle toward the personal best and global best positions. In reported works [16, 17], c_1 and c_2 were set in the range $[1, 2]$ and finally, from trial and error, the best choice of both is suggested to be 2.0 for each since it on average makes the weights for cognition and social parts to be 1.0. For the purpose of intending to simulate the slight unpredictable component of natural swarm behaviour, two random functions rand() are applied to independently provide uniform distributed numbers in the range [0, 1] to stochastically vary the relative pull of the personal and global best particles.

Step 4: Repeat Steps 2–3 until the algorithm stops.

3. APPLICATION TO DUALBAND CPW-FED ANTENNA DESIGN

The geometrical configuration of the candidate CPW-fed planar monopole antenna for achieving dualband operation is shown in Figure 1. For the proposed design here, the antenna is printed on only one side of an FR4 microwave substrate with the substrate thickness of 1.6 mm and the dielectric constant of 4.4. This construction is simpler than the presented dualband G-shaped antenna design, as reported in [21], which has a large ground plane on the side different from the G-shaped radiating patch. The main structure of the proposed antenna comprises two folded strips, denoted as L_1 and L_2, respectively, and a CPW feeding line. The strips L_1 and L_2 are both have a fixed strip width of s and are folded to resemble the antenna in a "G" shape. For the smaller folded strip L_1, it includes two horizontal sections with lengths of $w - w_f/2$ and ℓ_1 for the lower and upper sections, respectively, and one vertical section of length of $d_1 + s + s$. As for the larger folded strip, L_2, it includes two vertical and two horizontal sections, and can be determined by using only three parameters, which are the distances d_2 and d_3 from the upper horizontal section of the smaller folded strip to the left and right vertical section, respectively,

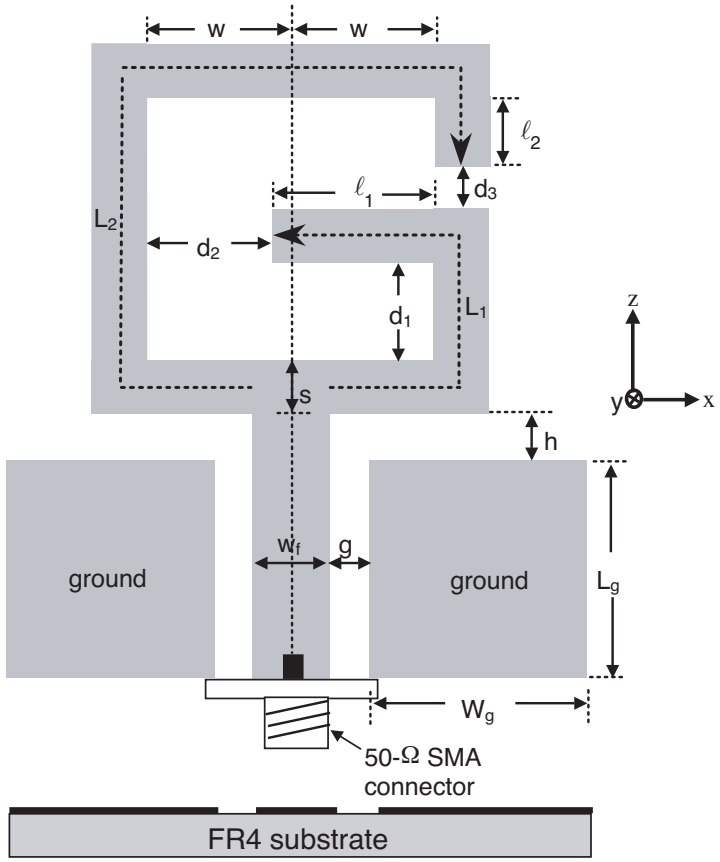

Figure 1. Geometrical configuration of proposed CPW-fed G-shaped monopole antenna for dualband.

of the larger folded strip, and the length ℓ_2 of the right vertical section of the larger folded strip. The major function of the two folded strips of unequal lengths is to produce two different current paths and thus expected to effectively excite dual resonant modes. A $50\,\Omega$ CPW feeding line with a fixed signal strip thickness of w_f and a gap distance of g between the signal strip and ground is used for centrally feeding the G-shaped antenna from its bottom edge. Two equal finite ground planes, each with dimensions of width W_g and length L_g, are situated symmetrically on each side of the CPW feeding line. The G-shaped radiating structure has a vertical spacing of h away from the ground plane. In this investigation, for trying to obtain good dualband impedance matching by controlling the current distribution

on the G-shaped stripline and compensation between the capacitive and inductive effects caused from the electromagnetic coupling effects of the finite ground planes and both the feeding line and the G-shaped stripline at the desired various operating bands, the geometry parameters of (ℓ_1, ℓ_2, d_1, d_2, d_3, s, w_f, W_g, L_g, g, h) will be optimally selected by the PSO. Note that the value of length w is determined by $(\ell_1 + d_2)/2$, thus it is not included in the design variables for use in the PSO optimization procedure. We defined eleven geometry parameters to compose a possible antenna design (i.e., a particle) and thereupon each of them was given appropriate minimum and maximum values as shown in Table 1. These parameters define an eleven-dimensional solution space in which the PSO searches for the optimal dualband CPW-fed antenna. For this case, we applied the "reflecting walls" technique, which indicates that when a particle hits the boundary of the solution space in any of the dimensions, the sign of the velocity in that dimension is changed and thus the particle is reflected back toward the solution space, to define the range of the particle's velocity in each dimension of the solution space. Afterwards, a selected population size of 30 particles is randomly generated initially. This number is suggested for most engineering problems [15] and has also been shown to be sufficient for our problem. On commencement of the iterations the so-called *fitness function* reflects the design goals is set to evaluate the fitness of each created particle for assessing its leadership among the swarm. The particle yielding the best objective function value will act as the swarm leader. Since the goal here is to achieve good impedance matching at the 2.45 and 5.2 GHz operating bands for suitable used 2.4/5.2 GHz WLAN applications, and in view of the wide variation of initial values obtained, the calculated return loss S_{11} at the above two operating frequencies were both normalized by an appropriate objective factor of -30 and -35 dB, respectively. The use of different factors for terms of 2.45 and 5.2 GHz is according to that for this antenna, the matching condition for operating at 2.45 GHz was

Table 1. Ranges of the design parameters for the dualband CPW-fed G-shaped monopole antenna.

Parameter	ℓ_1	ℓ_2	d_1	d_2	d_3	s	w_f	W_g	L_g	g	h
Range (mm)	0~15	0~15	0~15	0~15	0~15	1~5	2~5	5~20	5~20	0.2~5	0.2~6

found more difficult than that for operating at 5.2 GHz. However, the values of −30 dB and −35 dB should be good enough for impedance matching. As expected in such a multidimensional problem, numerical experiments showed that the two normalized terms made different contributions to the value of the fitness function. To prevent any of them from dominating the iteration process, each was weighted by an associated constant. In this example, we have found that the improvement of return loss at 2.45 GHz changed much more slowly than did the return loss at 5.2 GHz, so it must be more weighted. Thus weighting values of 0.75 and 0.25 were selected for 2.45 and 5.2 GHz terms, respectively, after a number of preliminary runs. This weighting technique effectively quickens the improvement of return loss at 2.45 GHz but slows that at 5.2 GHz. In addition, to ensure the algorithm quickly reaches to a solution of dualband operation a threshold of –10 dB return loss for each band was also set in the fitness function. The resulting fitness function was then:

$$fitness\ function = 0.75\frac{S_{11}(2.45\,\text{GHz})}{-30} + 0.25\frac{S_{11}(5.2\,\text{GHz})}{-35} + \sum_{i=1}^{2} G_i$$

$$G_i = \begin{cases} 1, & \text{if } S_{11}(f_i) \le -10 \text{ dB}, \\ 0, & \text{if } S_{11}(f_i) > -10 \text{ dB}. \end{cases}$$

$$i = 1 \text{ and } 2 \text{ for } 2.45 \text{ and } 5.2\,\text{GHz, respectively} \tag{3}$$

In addition, to avoid the solution's becoming stuck in a local pool we will put only −30 dB for 2.45 GHz term or −35 dB for 5.2 GHz term in the fitness function to evaluate the fitness once a return loss of less than −30 dB and −35 dB for operating at 2.45 GHz and 5.2 GHz, respectively, is achieved. Having defined the solution space and a fitness function, the task remains only to set the values of the learning parameters, such as w, c_1 and c_2, the stop criterion, and then run the PSO. For this case, we set the inertia weight factor (w) to vary linearly from 0.9 to 0.4 over 100 iterations, and the acceleration constants of c_1 and c_2 were both set to 2.0. Furthermore, a stop criterion was set arbitrarily to operate once the fitness function became asymptotic to its maximum value and remained so for at least 30 iterations. If the procedure does not stop, the modified velocity and position of each particle can be calculated using the current velocity and the distance from the stored individual's and global best positions. The algorithm runs through these processes iteratively until it converges.

4. RESULTS AND DISCUSSION

The progress of the PSO routine as a function of the number of iterations is revealed in Figure 2. Both return loss at 2.45 and 5.2 GHz and fitness of the best-designed antenna in each iteration are shown on the plot. The optimal G-shaped CPW-fed planar monopole antenna for dualband operation has reached after 56 iterations. It is clearly seen that improvement of return loss at 5.2 GHz is always better than that at 2.45 GHz during the optimization procedure. The PSO algorithm certainly created an optimal dualband antenna which has the following geometry parameters: $\ell_1 = 10\,\text{mm}$, $\ell_2 = 1.19\,\text{mm}$, d_1=10 mm, $d_2 = 3.32\,\text{mm}$, $d_3 = 10\,\text{mm}$, $s = 2.99\,\text{mm}$, $w_f = 4.75\,\text{mm}$, $W_g = 5\,\text{mm}$, $L_g = 10.75\,\text{mm}$, $g = 1.35\,\text{mm}$, and $h = 4.69\,\text{mm}$. The best-designed antenna was thus constructed and experimentally studied.

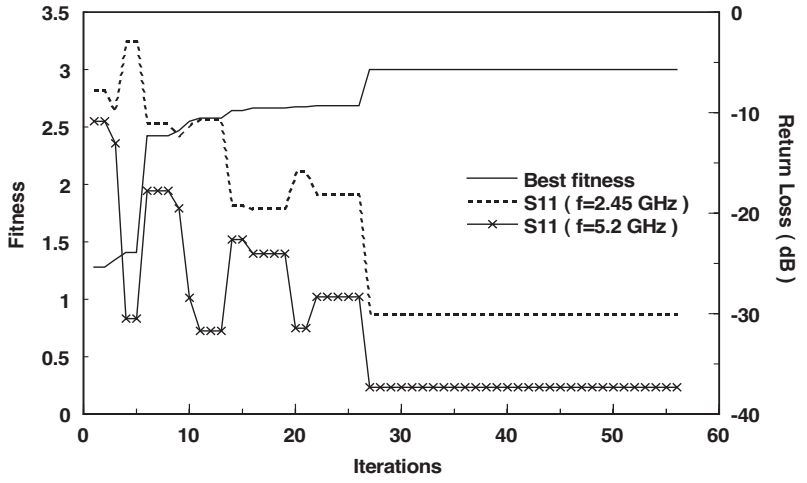

Figure 2. Fitness and return losses of the best-designed antenna in each iteration during the progress of the PSO algorithm.

Figure 3 shows the measurement and simulation frequency response of the return loss for the proposed antenna. Obviously, the simulation results show that except the two resonant modes at frequencies of 2.45 and 5.2 GHz, which are the same as those we put in the fitness function of the PSO process, two additional resonant modes are also excited at frequencies about 4.4 and 5.8 GHz. Especially, the simulated 10 dB impedance bandwidths across the three excited resonant bands at 4.4, 5.2, and 5.8 GHz are sufficient to produce a much broader continuous bandwidth from 3.91 to 6.46 GHz. As

for the measured results, also, four resonant modes at frequency of 2.43, 4.3, 5.24, and 6.09 GHz were obtained. The lower mode has an impedance bandwidth (10 dB return loss) of 236 MHz (2.3–2.536 GHz), or about 9.7% with respect to the centre frequency at 2.43 GHz, while for the higher mode, a broader continuous bandwidth produced from the three close resonant modes at 4.3, 5.24, and 6.09 GHz, has been reached to be 2.7 GHz (3.92–6.62 GHz), or about 62.8% referred to the best resonance frequency at 4.3 GHz. Obviously, the agreement between simulation and measurement seems very good. In addition, the obtained bandwidths can sufficiently cover the WLAN standards in the 2.4 GHz (2.4–2.484 GHz), 5.2 GHz (5.15–5.35 GHz), and 5.8 GHz (5.725–5.825 GHz) bands. Further, to examine the effects of the two folded-strip lengths of the proposed antenna on the impedance matching, the return loss response against frequency for the antenna with various lengths of ℓ_1 and ℓ_2 were also investigated.

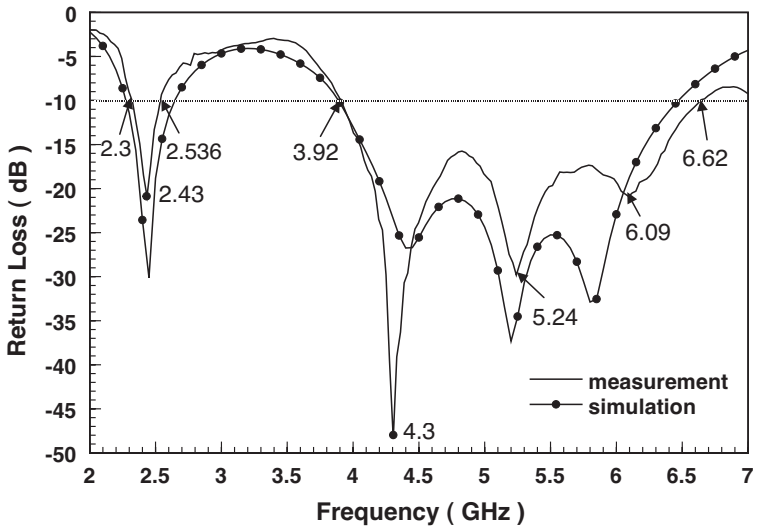

Figure 3. Return loss against frequency of proposed antenna from simulation and measurement: $\ell_1 = 10\,\text{mm}$, $\ell_2 = 1.19\,\text{mm}$, $d_1 = 10\,\text{mm}$, $d_2 = 3.32\,\text{mm}$, $d_3 = 10\,\text{mm}$, $s = 2.99\,\text{mm}$, $w_f = 4.75\,\text{mm}$, $W_g = 5\,\text{mm}$, $L_g = 10.75\,\text{mm}$, $g = 1.35\,\text{mm}$, and $h = 4.69\,\text{mm}$.

Figure 4 shows the simulated return loss of the proposed antenna with strip length ℓ_1=8, 10, and 12 mm, which results in the length of L_1 to be 28.27 mm, 30.27 mm, and 32.27 mm. Note that the strip length ℓ_1 of 10 mm is the obtained value for our optimized antenna as shown in Figure 3. It can be clearly seen that the resonant frequency

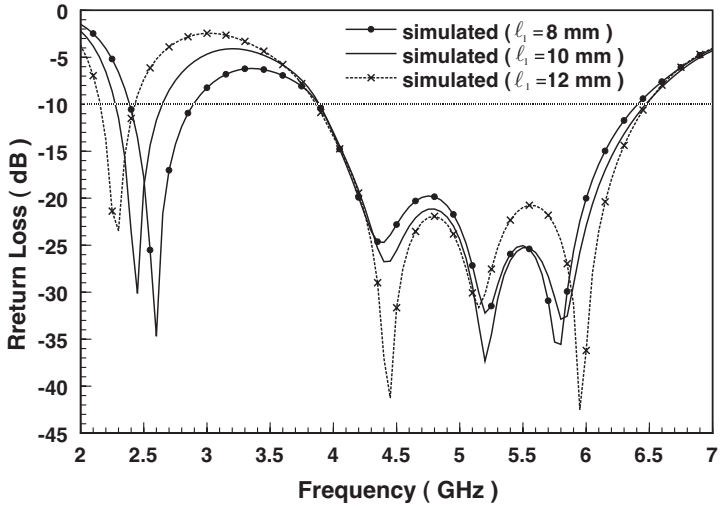

Figure 4. Simulated return loss against frequency for the proposed antenna with $\ell_1 = 8, 10, 12$ mm; other parameters are the same as in Figure 3.

of the lower band is changed, while the impedance matching for the higher band is only slightly affected. As the length ℓ_1 is increased, the lower resonant frequency is moved toward the lower frequency band. This result indicates that the smaller folded-strip path L_1 is considered to mainly control the lower operating band of the proposed antenna. For the optimized case (i.e., ℓ_1=10 mm), the electric length of L_1 is about 30.27 mm, which is almost equal to one-quarter wavelength of the operating frequency at 2.45 GHz, while the larger folded-strip path L_2 has an electrical length of 51.95 mm, which is about 0.9 λ of the higher operating frequency at 5.2 GHz. To further verify this, the tuning effects of the folded-strip length L_2 on impedance matching are also examined and shown in Figure 5. The selected strip length, ℓ_2, is from 0.69 to 1.69 mm with an increment of 0.5 mm, which results in the length of L_2 to be 51.45 mm, 51.95 mm, and 52.45 mm. Also note that the strip length, ℓ_2, of 1.19 mm is the dimension used for the obtained optimal design. Obviously, for the proposed design, varying the length of ℓ_2, as expected, does not significantly change the lower resonant mode but does affect the impedance matching condition of the higher operating band. It should be noted that for case of $\ell_2 = 1.69$ mm, though the obtained return loss at 5.2 GHz (about -52.32 dB) seems much higher than that in the optimized case (about -37.33 dB), the return loss at 2.45 GHz in former case (-28.71 dB)

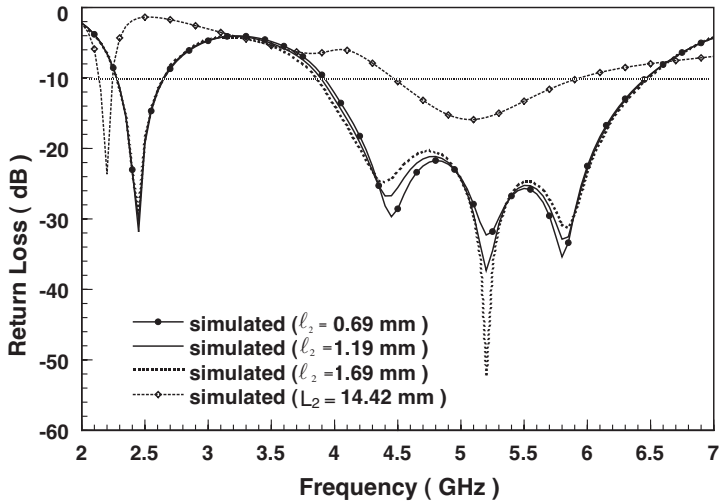

Figure 5. Simulated return loss against frequency for the proposed antenna with $\ell_2 = 0.69$ mm, 1.19 mm, 1.69 mm, and $L_2 = 14.42$ mm; other parameters are the same as in Figure 3.

is less than the later (-30.13 dB) to produce a less fitness than the optimal case of $\ell_2 = 1.19$ mm. In addition, we have also checked the case of decreasing the length of L_2 to be 14.42 mm, or about 0.25λ with respect to the operating frequency at 5.2 GHz, and select the other parameters as the optimized design. The calculated result shows that the dual resonant modes do occur at 2.2 and 5.1 GHz. The two frequencies both have a frequency shift to the desired operating bands of 2.45 and 5.2 GHz, respectively. The shifts may mainly due to the electromagnetic coupling effects between the folded strips L_1 and L_2. In addition, it can also be found that the impedance matching at 5.2 GHz band is much worse than that of the proposed optimal design. However, as the length of L_2 increases from 0.25λ to 0.9λ, the impedance bandwidth of the higher band is effectively increased. From these results, the dual-resonant modes for the proposed best-designed case can be concluded as that the lower operating mode is excited by the shorter folded-strip path L_1 with an appropriate length of 0.25λ, while the higher broad operating band is occurred from the formed longer current path L_2 with a length of 0.9 λ, respecting to the resonant frequency of 5.2 GHz.

Radiation characteristics of the optimised antenna are also studied. Figures 6–8 plot, respectively, the measured radiation patterns including the vertical (E_θ) and the horizontal (E_ϕ)

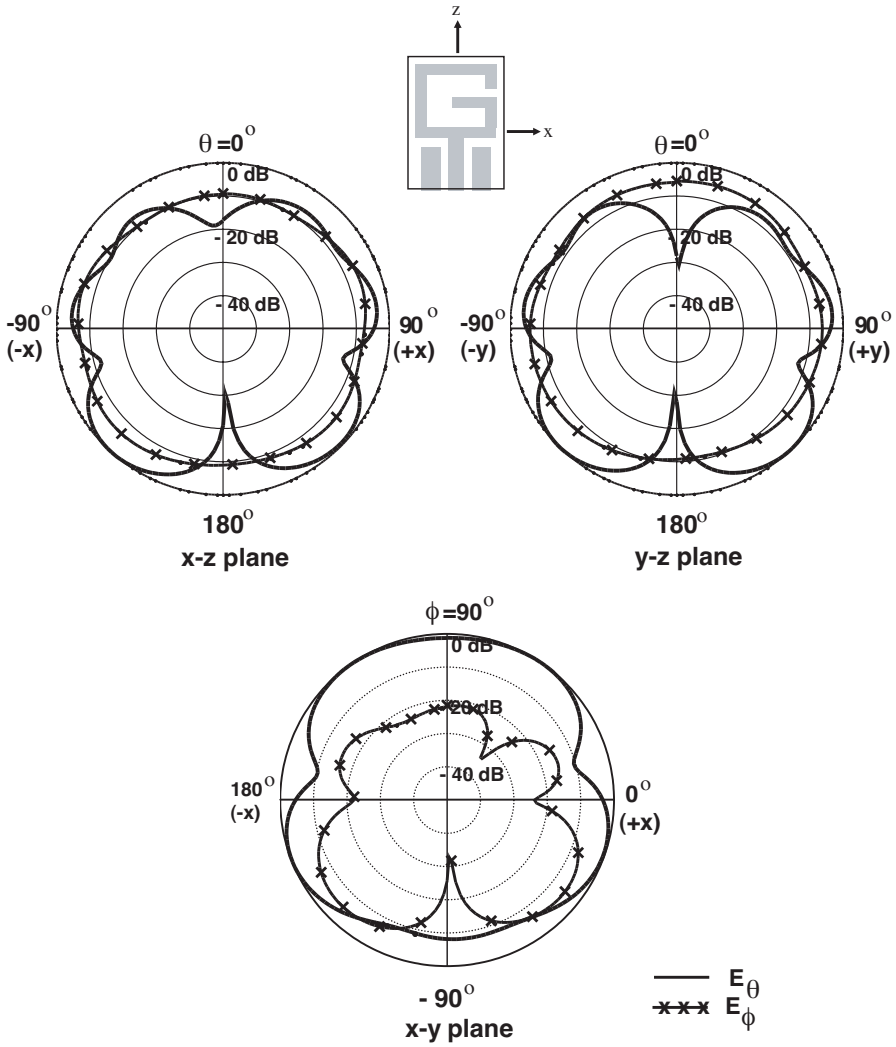

Figure 6. Measured radiation patterns at 2.45 GHz for the proposed antenna studied in Figure 3.

polarization patterns in the elevation direction (x-z and y-z planes) and azimuthal direction (x-y plane) at 2.45, 5.25, and 5.75 GHz for the proposed antenna. Due to the asymmetry in the G-shaped structure, unsymmetrical radiation patterns are seen in the three cuts as depicted in the plots. In addition, general monopole-like radiation patterns in the x-z and y-z planes and nearly omnidirectional radiation in the

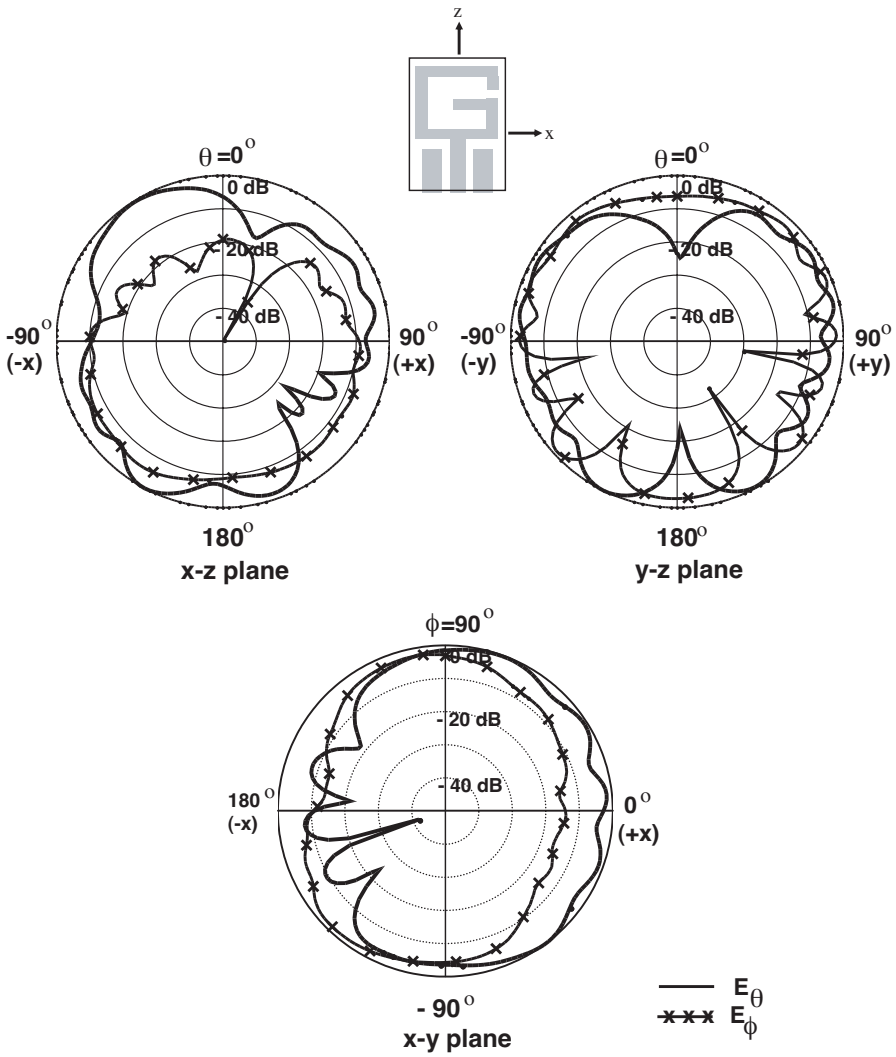

Figure 7. Measured radiation patterns at 5.25 GHz for the proposed antenna studied in Figure 3.

azimuthal plane are observed. However, it is also found that the E_θ and E_ϕ components of the patterns in both the x-z and y-z planes are seemed to be much comparable. This electromagnetic phenomenon is probably a result of the strong horizontal components of the surface current at the two folded-strip of the G-shaped structure. Also note

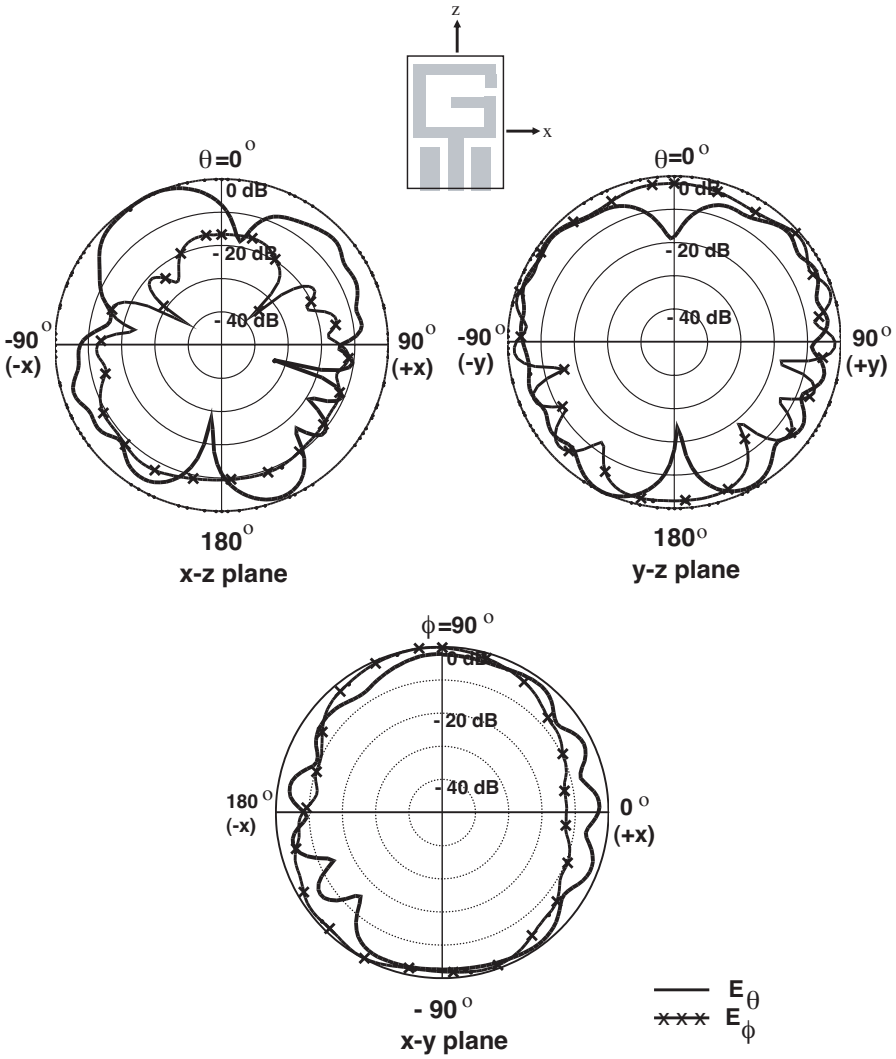

Figure 8. Measured radiation patterns at 5.75 GHz for the proposed antenna studied in Figure 3.

that very stable radiation patterns have been obtained for the proposed antenna from measurements at other operating frequencies across the bandwidth of each band. The peak antenna gain of the proposed antenna for frequencies across the dual bands was measured and shown in Figure 9. The ranges of antenna gain at the lower band of around

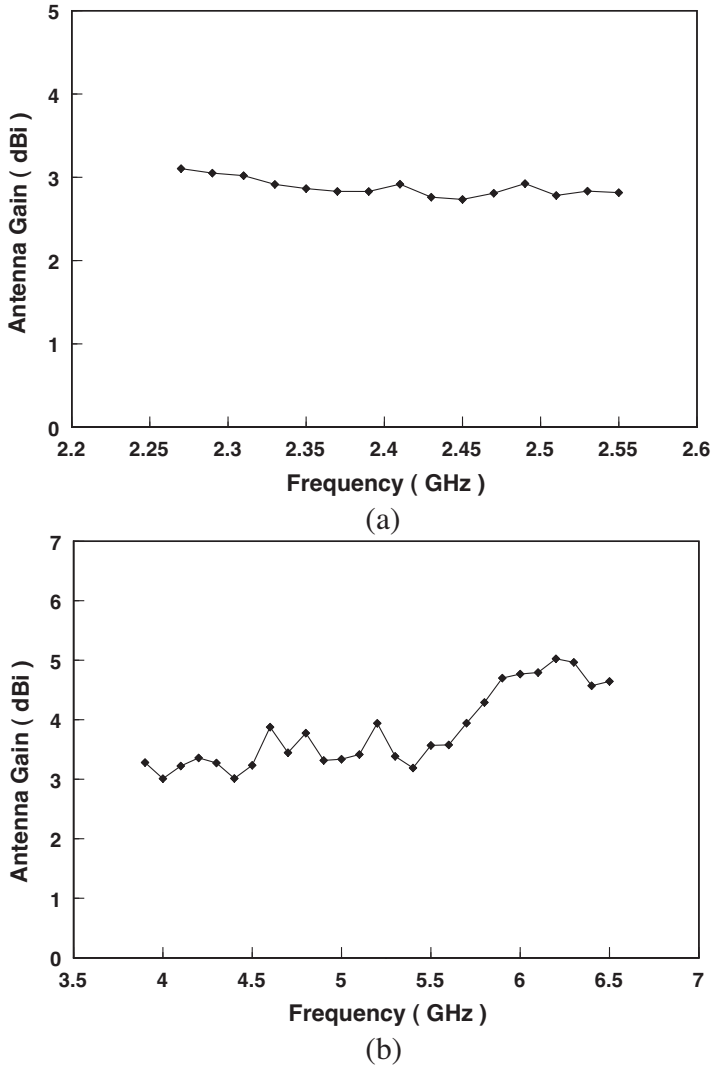

Figure 9. Measured peak antenna gain for frequencies across (a) the lower band (2.3–2.536 GHz) and (b) the higher band (3.92–6.62 GHz) for the proposed antenna studied in Figure 3.

2.45 GHz is about 2.7–3.1 dBi with a very flat gain curve, while that at the higher operating band ranged from 3.9 to 6.6 GHz is about 3–5 dBi also with a small gain variation around 5 GHz band.

5. CONCLUSION

In this paper, a novel CPW-fed G-shaped planar monopole antenna with dualband operation is presented. The design process used the particle swarm optimization to optimize the performance of the antenna by choosing the most appropriate configuration parameters. In addition to demonstrate in detail the application of the PSO optimization technique to this antenna design, constructed prototype of the PSO-resulted antenna with dual impedance bandwidths of 9.7% and 62.8% at bands of 2.43 and 4.3 GHz, respectively, sufficiently covering the bandwidth requirements of the WLAN system in the 2.4/5.2/5.8 GHz standards, have also been studied. Good antenna performances have been obtained and shown to match well with the numerical prediction.

ACKNOWLEDGMENT

This work was supported by the National Science Council of Republic of China under grant NSC 95-2221-E150-019.

REFERENCES

1. Song, C. T. P., P. S. Hall, H. Ghafouri-Shiraz, and D. Wake, "Triple band planar inverted F antennas for handheld devices," *Electron. Lett.*, Vol. 36, 112–114, 2002.
2. Hsiao, F. R. and K. L. Wong, "Compact planar inverted-F patch antenna for triple-frequency operation," *Microw. Opt. Technol. Lett.*, Vol. 33, 459–462, 2002.
3. Dou, W. P. and Y. W. M. Chia, "Novel meandered planar inverted-F antenna for triple-frequency operation," *Microw. Opt. Technol. Lett.*, Vol. 27, 58–60, 2000.
4. Dakeya, Y., T. Suesada, K. Asakura, N. Nakajima, and H. Mandai, "Chip multiplayer antenna for 2.45 GHz-band application using LTCC technology," *IEEE MTT-S Int. Microw. Symp. Dig.*, 1693–1696, 2000.
5. Choi, W., S. Kwon, and B. Lee, "Ceramic chip antenna using meander conductor lines," *Electron. Lett.*, Vol. 37, 933–934, 2001.
6. Eldek, A. A., A. Z. Elsherbeni, and C. E. Smith, "Square slot antenna for dual wideband wireless communication systems," *Journal of Electromagnetic Waves and Applications*, Vol. 19, 1571–1581, 2005.

7. Lee, E., P. S. Hall, and P. Gardner, "Compact wideband planar monopole antenna," *Electron. Lett.*, Vol. 35, 2157–2158, 1999.
8. Wong, K. L., G. Y. Lee, and T. W. Chiou, "A low-profile planar monopole antenna for multiband operation of mobile handsets," *IEEE Trans. Antennas Propagat.*, Vol. 51, 121–124, 2003.
9. Saed, M. A., "Broadband CPW-fed planar slot antennas with various tuning stubs," *Progress In Electromagnetics Research*, PIER 66, 199–212, 2006.
10. Raj, R. K., M. Joseph, B. Paul, and P. Mohanan, "Compact planar multiband antenna for GPS, DCS, 2.5/5.8 GHz WLAN applications," *Electron. Lett.*, Vol. 41, 290–291, 2005.
11. Liu, W. C. and C. F. Hsu, "CPW-fed notched monopole antenna for UMTS/IMT-2000/WLAN applications," *Journal of Electromagnetic Waves and Applications*, Vol. 21, 841–851, 2007.
12. Liu, W. C., "Broadband dual-frequency meandered CPW-fed monopole antenna," *Electron. Lett.*, Vol. 40, 1319–1320, 2004.
13. Davis, L., *Genetic Algorithms and Simulated Annealing*, Pittman, London, U.K., 1987.
14. Liu, W. C., "Design of a CPW-fed notched planar monopole antenna for multiband operations using a genetic algorithm," *IEE Proc. Microw. Antennas Propagat.*, Vol. 152, 273–277, 2005.
15. Kennedy, J. and R. C. Eberhart, "Particle swarm optimization," *Proc. IEEE Conf. Neural Networks IV*, Piscataway, NJ, 1995.
16. Robinson, J. and Y. Rahmat-Samii, "Particle swarm optimization in electromagnetics," *IEEE Trans. Antennas Propagat.*, Vol. 52, 397–407, 2004.
17. Liu, W. C., "Design of a multiband CPW-fed monopole antenna using a particle swarm optimization approach," *IEEE Trans. Antennas Propagat.*, Vol. 53, 3273–3279, 2005.
18. Lee, K. C. and J. Y. Jhang, "Application of particle swarm algorithm to the optimization of unequally spaced antenna arrays," *Journal of Electromagnetic Waves and Applications*, Vol. 20, 2001–2012, 2006.
19. Chen, T. B., Y. L. Dong, Y. C. Jiao, and F. S. Zhang, "Synthesis of circular antenna array using crossed particle swarm optimization algorithm," *Journal of Electromagnetic Waves and Applications*, Vol. 20, 1785–1795, 2006.
20. Mahmoud, K. R., M. El-Adawy, S. M. M. Ibrahem, R. Bansal, and S. H. Zainud-Deen, "A comparison between circular and hexagonal array geometries for smart antenna systems using particle swarm optimization algorithm," *Progress In Electromagnetics Research*,

PIER 72, 75–90, 2007.

21. Pan, C. Y., C. H. Huang, and T. S. Horng, "A new printed G-shaped monopole antenna for dualband WLAN applications," *Microw. Opt. Technol. Lett.*, Vol. 45, 295–297, 2005.